Diradicals

Deutsche Ausgabe: DOI: 10.1002/ange.201607415
Internationale Ausgabe: DOI: 10.1002/anie.201607415

A Thermally Populated, Perpendicularly Twisted Alkene Triplet Diradical

Curt Wentrup, Michèle J. Regimbald-Krnel, Dennis Müller, and Peter Comba*

Abstract: *Variable-temperature NMR and ESR spectroscopic studies reveal that bis(dibenzo[a,i]fluorenylidene) **1** possesses a singlet ground state, **1**(S_0), while the 90° twisted triplet **1**(T_1) is populated to a small extent already at room temperature. Analysis of the increasing amount of paramagnetic **1**(T_1) at temperatures between 300 and 500 K yields the exchange interaction $J_{ex}/hc = 3351\ cm^{-1}$ and a singlet–triplet energy splitting of 9.6 kcal mol^{-1}, which is in excellent agreement with calculations (9.3 kcal mol^{-1} at the UKS BP86/B3LYP/revPBE level of theory). In contrast, the zero-field splitting parameter D is very small (calculated value −0.018 cm^{-1}) and unmeasurable.*

Diradicals have fascinating physical and chemical properties.[1] It is well known that simple alkenes have barriers of rotation about the C=C bond on the order of 65 kcal mol^{-1}, and a recent study of the singlet–triplet gap in ethylene yielded a similar value of 58 ± 3 kcal mol^{-1}.[2] Steric hindrance can dramatically lower this barrier; a barrier as low as 6.4 kcal mol^{-1} has been calculated for experimentally unknown tetra-*tert*-butylethene at the B3LYP/6-311 + G-(2d,p) level of theory.[3] Very recently, a triplet diradical arising from the twisted Si=Si bond in tetrakis(di-*tert*-butylmethylsilyl)disilene with a singlet–triplet splitting of 7.3 kcal mol^{-1} was described.[4]

Dark-green, overcrowded 13,13′-bis(dibenzo-[*a,i*]fluorenylidene) (**1**), which was first described in 1925,[5] is no less fascinating (Scheme 1). Obviously, steric strain prevents this compound from being planar. A single-line ESR spectrum ascribed to **1** has been reported, and the energy difference between the singlet ^{1}**1** (S_0) and the triplet ^{3}**1** (T_1) has been estimated to be approximately 4 kcal mol^{-1} based on changes in the UV/Vis spectrum ($\lambda_{max} = 623$ nm) in the 293–123 K range.[6] The X-ray crystal structure of **1**($_0$) features a torsion angle of 52° between the two nearly planar halves of the molecule.[7] The central C13=C13′ distance is 140.8 pm. The bending angles at the central C=C bond are 0.7 and 2.1°; thus the compound is twisted but only slightly bent. For comparison, in the red bifluorenylidene **2a**, the central C=C bond length is 136 pm, the twist angle in pyrene is 39°,[8] and $\lambda_{max} = 458$ nm.[9] The barrier to rotation about the C=C bond in 2,2′-dimethylbifluorenylidene (**2b**) is 25 kcal mol^{-1}, and a very similar barrier is expected for **2a**.[10] In (*E*)-bis(benzo-[*a*]fluorenylidene) ((*E*)-**3**), the central C=C bond is 138.6 pm long, the twist angle is 39°, $\lambda_{max} = 507$ nm, and the calculated rotational barrier amounts to 20 kcal mol^{-1}.[11] In the more severely hindered *Z* isomer (*Z*)-**3**, the barrier is 14 kcal mol^{-1}. The structures, twisting and folding angles, and barriers to rotation of several sterically crowded bifluorenylidene and bianthrone derivatives have been reviewed.[12] The hindered rotation in overcrowded alkenes has been used by Feringa et al. in the construction of molecular machines.[13] Furthermore, large, planar, polycyclic hydrocarbons with singlet–triplet gaps of 1–4 kcal mol^{-1} were recently reported.[14,15]

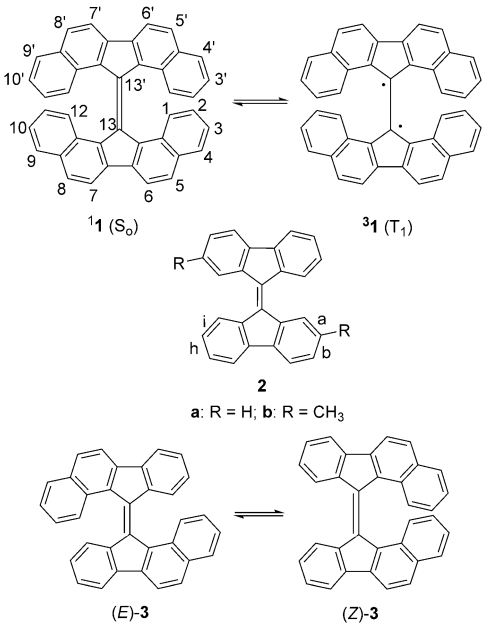

Scheme 1. Singlet and triplet bis(dibenzo[*a,i*]fluorenylidene) **1**, bifluorenylidenes **2**, and bis(benzo[*a*]fluorenylidene) **3**.

No further experimental investigations of **1** have been reported, but Lenoir et al. recently published calculations at the UB3LYP/6–311 + G(2d,p) level of theory and obtained a singlet–triplet splitting of 3.4 kcal mol^{-1} (ΔH_{ST} in the gas phase) and torsional angles of 53° in the ground-state singlet **1**(S_0) and 90° in the triplet **1**(T_1).[3] The corresponding calculated values for bifluorenylidene **2** at the same level of theory are 19.5 kcal mol^{-1}, 34° (S_0), and 90° (T_1).[3]

[*] Prof. Dr. C. Wentrup, Dr. M. J. Regimbald-Krnel
School of Chemistry and Molecular Biosciences
The University of Queensland
Brisbane, Queensland 4072 (Australia)
E-mail: wentrup@uq.edu.au
Homepage: http://researchers.uq.edu.au/researcher/3606
Dr. D. Müller, Prof. Dr. P. Comba
Anorganisch-Chemisches Institut and IWR
Universität Heidelberg
Im Neuenheimer Feld 270, 69120 Heidelberg (Germany)
Supporting information and the ORCID identification number(s) for the author(s) of this article can be found under: http://dx.doi.org/10.1002/anie.201607415.

Herein, we report our NMR and ESR studies of bis-(dibenzo[*a*,*i*]fluorenylidene) (**1**), which support the notion of a thermally populated triplet state **1**(T_1) arising from torsion around the C=C bond in the twisted ground state **1**(S_o). Variable-temperature ESR experiments revealed a very strong antiferromagnetic exchange interaction J_{ex}, leading to a singlet–triplet splitting of about 9.6 kcal mol^{-1} and a very small zero-field splitting parameter *D*.

Temperature-dependent ^{1}H and ^{13}C NMR spectra of **1** reveal noticeable line broadening already at room temperature, and this becomes more severe as the temperature is increased to 400 K (Figures 1 and 2). Conversely, all resonances sharpen upon decreasing the temperature to 233 K (see the Supporting Information, Figures S1–S3). All proton and carbon resonances were assigned with the aid of COSY, HSQC, and HMBC ^{1}H–^{1}H and ^{1}H–^{13}C 2D correlations.

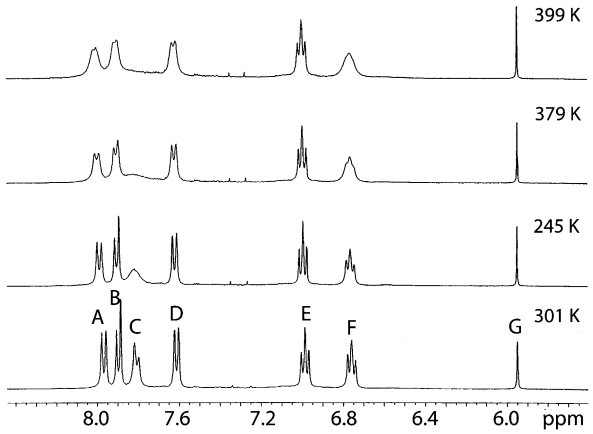

Figure 1. Variable-temperature ^{1}H NMR spectra (400 MHz) of **1** in 1,1,2,2-tetrachloroethane-d_2. A = H1/H1′/H12/H12′ (δ = 8.0), B = H6/H6′/H7/H7′ (7.9), C = H5/H5′/H8/H8′ (7.8), D = H4/H4′/H9/H9′ (7.6), E = H3/H3′/H10/H10′ (7.0), F = H2/H2′/H11/H11′ (6.8), G = $(CHCl_2)_2$ (5.9 ppm).

In the ^{1}H NMR spectrum, the doublet at 7.8 ppm (C), which is due to H5/H5′/H8/H8′, is affected most, followed by the triplet at 6.8 ppm (F), which corresponds to the H2/H2′/H11/H11′ protons (Figure 1). In the ^{13}C NMR spectrum, the lowest-field resonance at 148 ppm (A; C13/C13′) is very weak and broad at room temperature, and the carbon atoms belonging to the aromatic rings closest to the olefinic C=C bond are more affected than those on the outer rings (Figure 2).

The presence of unpaired electrons results in broadened NMR resonances owing to increased relaxation rates.[16,17] Lowering the temperature decreases the population of the triplet state of **1**. At 233 K (−40 °C), most of **1** is now in the singlet state, the sample is almost completely diamagnetic, and sharp NMR resonances are observed (Figures S2 and S3). Nine principal canonical structures can be formulated for the triplet diradical ^{3}**1**(T_1) (Scheme S1). The spin density is expected to be the highest on the ethylenic carbon atoms C13/C13′ because in this canonical structure, all eight benzene rings are in the Kekulé form, and this was confirmed by

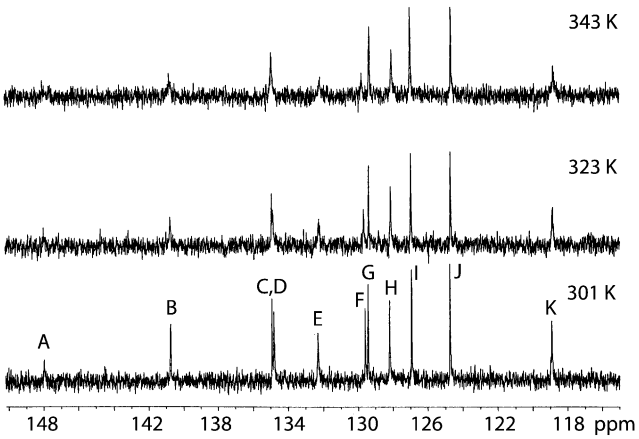

Figure 2. Variable-temperature ^{13}C NMR spectra (100 MHz) of **1** in 1,1,2,2-tetrachloroethane-d_2. A = C13/C13′ (δ = 147.9), B = C6a/C6a′/C6b/C6b′ (140.6), C = C12b/C12b′/C13a/C13a′ (134.9), D = C4a/C4a′/C8a/C8a′ (134.7), E = C5/C5′/C8/C8′ (132.0), F = C12a/C12a′/C13b/C13b′ (129.6), G = C4/C4′/C9/C9′ (129.1), H = C2/C2′/C11/C11′ (127.8), I = C1/C1′/C12/C12′ (126.8), J = C3/C3′/C10/C10′ (124.5), K = C6/C6′/C7/C7′ (118.5 ppm).

calculations (see Tables S2–S5). There are two resonance structures with only seven benzenoid rings in the Kekulé form (with spin densities at C13 and C5/C6a′), three with six benzenoid Kelulé rings (with spin densities at C13 and C2′/C4′/C13b′), and three with five benzenoid Kekulé rings (with spin densities on C13 and C1′/C3′/C6′). This ranking also agrees well with the spin densities previously[3] calculated for ^{3}**1** and in the current work (Table S6): C13 (0.34) > C5/C8 (0.17) > C2/C11 (0.05) = C4/C9 (0.05) > C1/C3/C6/C7/C10/C12 (−0.02).

Thus the experimental observation that the resonance for C13/C13′ (A, 148 ppm) is already significantly broadened at room temperature, followed by those corresponding to C5/C5′/C8/C8′ (E, 132 ppm) and C6a/C6a′/C6b/C6b′ (B, 141 ppm; Figure 2), is in excellent agreement with expectations from spin-density considerations. The resonance for C12b/C12b′/C13a/C13a′ (C, 134.9 ppm) has also broadened and merged with that for C4a/C4a′/C8a/C8a′ at 343 K (D, 134.7 ppm). The observed line broadening is ascribed to the increased population of the paramagnetic triplet state **1**(T_1) at elevated temperatures.

Solid-state ESR spectroscopy of **1** confirmed its paramagnetic nature, yielding a single resonance at g = 0.0279 (Figure 3 b). Cooling from room temperature to 136 K caused a decrease in the signal intensity (Figure 3 a). Similar spectra were obtained for a 1.2×10^{-3} M solution of **1** in benzene. In agreement with the NMR observations, the signal was no longer observable at 77 K. Conversely, heating to 500 K caused a continuous increase in the signal intensity (Figures S8–S10).

The spin Hamiltonian describing a spin-coupled system of two electrons includes contributions from through-space dipole–dipole interactions H_{dip} and a scalar exchange interaction H_{ex}, where H_{dip} is inversely proportional to the third power of the average dipole–dipole distance *r* and also depends on the angle between the vector **r** and the direction

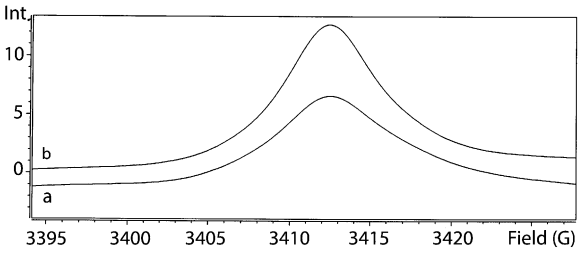

Figure 3. Continuous-wave solid-state X-band ESR absorption spectra of **1** at a) 136 K and b) 295 K. $\nu = 9.5655$ GHz, $g = 2.00279$. Ordinate: intensity in arbitrary units. For the first derivative spectra, see Figure S7.

of the external magnetic field.[18] The dipolar interaction is governed by the zero-field operator **D** according to $S\cdot\mathbf{D}\cdot S = D(S_z^2 - 1/3\,S(S+1)) + E(S_x^2 - S_y^2)$, where D and E are the zero-field splitting parameters, and S is the total spin. The selection rule $\Delta m_s = \pm 1$ predicts two ESR transitions, but the dipole–dipole coupling vanishes when the angle between the orbitals is 90°, as is the case for the SOMOs in ^{3}**1** (see Figures 4, S13, and S14), with the consequence that the ESR spectrum will consist of a single resonance as if it were due to a doublet monoradical, and D becomes unmeasurably small. Other recently reported hydrocarbon diradicals also show only a single resonance at $g \approx 2$,[14,15,19,20] but here the small value of D is more likely due to extensive delocalization.[21]

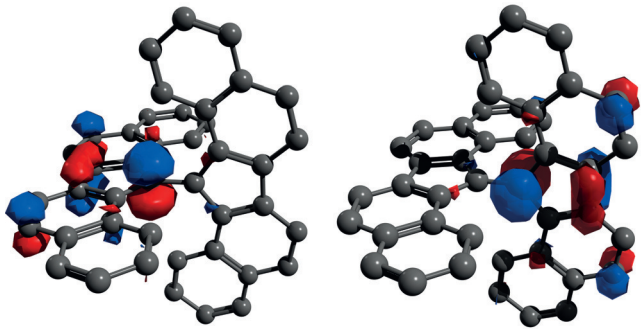

Figure 4. SOMOs of 90° twisted ^{3}**1**(T_1) at the UKS BP86/def2-TZVP level of theory (isovalue = 0.05). Note the significant spin densities at C5 and C8, which are in agreement with the expectations from the ^{1}H NMR data.

The electronic structures of the singlet and triplet states of **1** were optimized using the ORCA 3.0.3 program[22] at the UKS BP86/B3LYP/revPBE level of theory[23] with the def2-TZVP basis set.[24] The D3 dispersion correction[25] was also accounted for, and numerical frequencies were calculated for the BP86 and revPBE functionals. The zfs parameters D and E were calculated at the UKS BP86/EPR-II level of theory, yielding $E/hc^{calc} = 0.000\ cm^{-1}$. The calculation of D indicates partial cancellation of the spin–spin and spin–orbit contributions, which amount to -0.03620 and $0.018\ cm^{-1}$, respectively. Thus the total D/hc^{calc} value equals $-0.018\ cm^{-1}$ (Table S5). This computational method is known to give good agreement with experimental values for organic radicals.[26]

The forbidden $\Delta m_s = \pm 2$ transition also depends on the magnitude of the dipole–dipole coupling,[18] and such a transition was not observed for **1** either in benzene solution or in the solid state up to 370 K.

The exchange coupling H_{ex} of the two unpaired electrons takes place through the overlap of molecular orbitals and is characterized by the exchange integral J_{ex}. The energies E of the singlet ($S = 0$) and triplet ($S = 1$) states are given[18a] by Equation (1),

$$E(S) = {}^1/_2 J_{ex}[S(S+1) - S_1(S_1+1) - S_2(S_2+1)] \quad (1)$$

from which it follows that the singlet–triplet energy separation ΔE_{ST} equals J_{ex}. When the singlet is the ground state and the triplet is thermally populated, the coupling is antiferromagnetic.[18a] The ESR signal intensity I of the coupled triplet state is temperature-dependent according to the Boltzmann law [Eq. (2)],[18a,27]

$$I_{S=1} = Ce^{-E(S)/kT}/Z \quad (2)$$

where C is a constant, k is the Boltzmann constant, Z is the partition function,

$$Z = \sum_{S=0}^{1} (2S+1)e^{-E(S)/kT} \quad (3)$$

and $E(S)$ is given by Equation (1). Therefore, the value of J_{ex} can be determined by variable-temperature measurements. Plots of the calculated signal intensity versus temperature for $J_{ex}/hc = 900$ and $3351\ cm^{-1}$ are given in Figures S11 a and S12. Increasing the temperature increases the population of the triplet and results in a more intense ESR signal, as observed for **1** in Figure 3 and Figures S8–S10. Once population of the $S = 1$ state is saturated, the intensity of the ESR signal will decrease upon a further increase in temperature according to the Curie law (Figure S11 a).[15] In contrast, in the absence of exchange coupling ($J_{ex} = 0$), the intensity will always follow the Curie law (Figure S11 b).

Variable-temperature ESR measurements on solid **1** showed that the signal intensity increased only slowly up to about 400 K (Figure S10), thus suggesting that the early part of the simulated plots in Figures S11 a and S12 was being followed. A variable-temperature experiment in the range of 420–500 K enabled the determination of J_{ex}.

The ESR signal intensity of solid **1** remained constant for at least 1 h at 420 K (Table S1). When the temperature was increased to 430 K, the signal intensity increased to a new constant value, and the same occurred on further temperature increases to 472 K and then to 500 K in 5 K intervals.

Figure 5 shows the experimental signal intensities together with the theoretical fit according to Equation (2). The curve fit in the range of 420–500 K yields a value of $J_{ex}/hc = 3351\ cm^{-1}$ or $J_{ex} = \Delta E_{ST} = 9.6\ kcal\,mol^{-1}$ for solid **1**.

However, when the temperature was increased above 500 K, the signal intensity was no longer constant but kept increasing with time (30% in 2 h), and similar increases were observed at 513 and 520 K (Figure S10 and Table S1). Therefore, the triplet state of **1** is no longer in thermodynamic

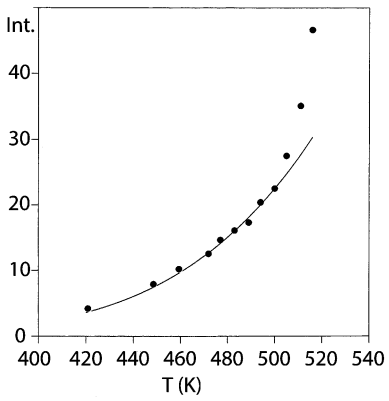

Figure 5. ESR signal intensity (Int., arbitrary units) for **1** as a function of temperature between 420 and 520 K. The solid line is the theoretical fit according to Equation (2).

equilibrium at temperatures above 500 K, and the data points above 500 K no longer follow the theoretical curve in Figure 5.

Thus the triplet state **1**(T_1) is stable up to 500 K, but at temperatures above 500 K, irreversible formation of a new, persistent paramagnetic species, presumably a monoradical, is taking place. When these samples were cooled again, the signal remained several times stronger than that observed before the heating process, and it did not return to the original value measured for **1** at 300 K (Figures 6, S9, and S10).

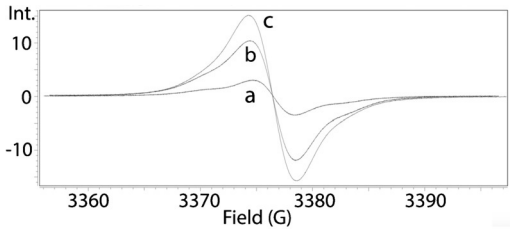

Figure 6. ESR spectrum of **1** in the solid state at a) 300 K before heating, b) 300 K after heating to 530 K and re-cooling, and c) 530 K. $\nu = 9.4676$ GHz.

The ^{1}H NMR spectrum of the heated and re-cooled sample revealed that none of the original compound **1** remained in the now brown material. Dibenzo[*a*,*i*]fluorene was isolated as one of several decomposition products. In another experiment, heating a solution of **1** in diphenyl ether at 473–503 K for 2.5 hours resulted in about 5% decomposition as measured by the absorbance at 632 nm. The persistent radical may be due to hydrogen abstraction at C13 of **1** forming a 13-(13′-dibenzo[*a*,*i*]fluorenyl)dibenzo-[*a*,*i*]fluoren-13-yl radical (Scheme S2). Sakurai et al.[28] have reported analogous persistent doublet free radical formation upon heating tetrakis(trimethylsilyl)ethylene to about 425 K, which is presumably formed by hydrogen abstraction by the triplet disilene, and Apeloig et al.[3] also reported the formation of a polysilyl doublet radical as a side product at 400 K.

The data described above imply that J_{ex} should be determined at as high a temperature as possible, but not above 500 K, and using the shortest practical measuring time in the higher temperature range. Estimates of J_{ex} and hence of the singlet–triplet splitting obtained from intensity measurements in the lower temperature range are less accurate. Franzen and Joschek[6] used small intensity differences in the visible spectrum in the range 293–423 K to estimate an energy difference of 4 kcal mol^{-1} for **1** in toluene solution. The value of 3.4 kcal mol^{-1} reported by Lenoir et al. was calculated for the gas phase.[3]

The J_{ex} value obtained for **1** demonstrates very strong through-bond electron exchange coupling. For comparison, the two Cu^{II} ions in di-μ-pyridine-*N*-oxide bis[dichloro aquo copper(II)] are strongly antiferromagnetically coupled with a J_{ex}/hc value of 885 cm^{-1}.[18a,29] The exchange interactions in organic diradicals are usually much smaller.[30,31] The large value of J_{ex} for **1** can be ascribed to the fact that the unpaired electrons are largely localized on the carbon atoms of the central C13=C13′ bond (see Figure 4 and Table S4) as confirmed by the NMR experiments reported above.

The singlet–triplet splitting ΔE_{ST} was calculated at several levels of theory (Table 1). The BP86 functional shows the best agreement with experiment, yielding $\Delta E_{ST} = 9.3$ kcal mol^{-1}, a C13=C13′ bond length in the singlet state **1**(S_0) of 140.9 pm, and a dihedral angle between the two halves of 49.7° (Table S3). The significant deviation from the previous DFT calculation of ΔE_{ST} (3.4 kcal mol^{-1})[3] is attributed in large part to the D3 dispersion correction, which stabilizes the singlet state more than the triplet state by about 4 kcal mol^{-1} owing to their structural differences.

Table 1: Experimental (ESR) and calculated singlet–triplet splittings and *g* values for **1**.

Method	ESR	BP86[a]	revPBE[a]	B3LYP[b]
ΔE_{ST} [kcal mol^{-1}]	9.6	9.3	8.7	7.1
g	2.0028	2.0026	2.0026	2.0027

[a] Gibbs free energy at 298.15 K. The single-point energies for BP86 and revPBE are 9.8 kcal mol^{-1} and 9.1 kcal mol^{-1}, respectively. [b] Single-point energy; no numerical frequencies were calculated.

To gain insight into the factors affecting the stabilization of triplet **1**, further calculations on isomer **4**[12] and the tetradecahydro model compound **5** were performed at the UKS BP86/def2-TZVP (D3BJ) level of theory (Figure 7 and Tables S2–S10).

For compound **4**, we calculated ΔE_{ST} to be 17.9 kcal mol^{-1}. However, the energy difference between the two triplet states

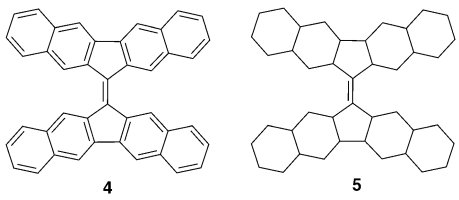

Figure 7. Isomer **4**[12] and model compound **5**.

of **1** and **4** is only 0.4 kcal mol^{-1} at a torsional angle of 90°, which is well within the error of the computation method. Thus the energy of the triplet **1**(T_1) does not depend on ground-state steric strain[12] (but its accessibility does, see below). For the singlet states ^{1}**1** and ^{1}**4** with a twisting angle of 49.7° (the optimized, calculated value for ^{1}**1**), the energy of ^{1}**4** is lower than that of ^{1}**1** by 8.2 kcal mol^{-1}. This therefore is a good estimate of the steric strain energy in compound **1** (note that 8.2 + 9.3 (ΔE_{ST} in **1**) = 17.5 ($\approx \Delta E_{ST}$ in **4**)).

Model compound **5** has a normal olefinic S–T splitting of 62.0 kcal mol^{-1} and a torsional angle of 35° in the ground state (see Scheme S3). Therefore, although the structures of **4** and **5** are obviously different (Scheme S3), it can be concluded that the aromatic delocalization is the major factor stabilizing the triplet state ^{3}**1** (by about 45 kcal mol^{-1}) together with the steric destabilization of the singlet ground state (ca. 8 kcal mol^{-1}). Nonetheless, the strain energy of 8 kcal mol^{-1} is highly important in making the S–T gap sufficiently small so that ^{3}**1** becomes observable at reasonable temperatures.

The larger calculated S–T gap in **4** (17.9 kcal mol^{-1}) means that forbiddingly high temperatures would be required to observe the ESR spectrum of ^{3}**4**, or else about 8 kcal mol^{-1} of extra steric strain would have to be introduced in the ground state ^{1}**4**.

The influence of torsion about the central C13–C13′ bond in **1** on the S–T gap was evaluated by carrying out single-point calculations of the singlet and triplet energies at the optimized triplet structure for various torsional angles. As expected, the larger the torsional angle, the smaller $\Delta E_{S\text{-}T}$, which approaches zero when the torsional angle approaches 90° (Table S2 and Figure S16). Thus, twisting, which is caused by steric crowding, lowers the singlet–triplet gap, but it is mainly delocalization in the resulting triplet diradical that lowers the energy of the triplet state and makes it accessible.

In conclusion, line broadening and the effects of temperature on the ^{1}H and ^{13}C NMR spectra of **1** indicate the presence of a thermally populated paramagnetic triplet state ^{3}**1** (T_1), whose amount increases with temperature. ESR spectroscopic studies revealed that the singlet state ^{1}**1** (S_0) is in equilibrium with the thermally populated antiferromagnetically coupled triplet ^{3}**1** (T_1) at 300–500 K. The dipole–dipole interaction in ^{3}**1** (T_1) is negligible, and consequently, the zero-field splitting parameter D is very small. In contrast, the exchange interaction J_{ex} is strong, and a value of $J_{ex}/hc = 3351$ cm^{-1}, which is equivalent to a singlet–triplet splitting ΔE_{ST} of 9.6 kcal mol^{-1}, in the solid state was derived. DFT calculations are in good agreement with experiment with $\Delta E_{ST}^{calc} \approx 9.3$ kcal mol^{-1} and $D/hc \approx 10^{-2}$ cm^{-1}. The low ΔE_{ST} value is due to a combination of ground-state steric strain and stabilization of the excited triplet state by delocalization. Compound **1** decomposes at temperatures above 500 K with formation of a persistent doublet monoradical.

Acknowledgements

M.J.R-K. is indebted to the Natural Science and Engineering Research Council of Canada for a Scholarship and to The University of Queensland (UQ) for an Overseas Postgraduate Research Scholarship. We are indebted to the late Professor Graeme R. Hanson, Centre for Analytical Imaging at UQ, for advice on and assistance with ESR spectroscopy.

Keywords: diradicals · exchange coupling · singlet–triplet splitting · strained molecules · twisting

How to cite: *Angew. Chem. Int. Ed.* **2016**, *55*, 14600–14605
Angew. Chem. **2016**, *128*, 14820–14825

[1] M. Abe, *Chem. Rev.* **2013**, *113*, 7011–7088.
[2] F. Qi, O. Sorkbati, A. G. Suits, S. H. Chien, W. K. Li, *J. Am. Chem. Soc.* **2001**, *123*, 148–161.
[3] B. Kanawati, A. Genest, P. Schmitt-Kopplin, D. Lenoir, *J. Mol. Model.* **2012**, *18*, 5089–5096.
[4] A. Kostenko, B. Tumanskii, M. Karni, S. Inoue, M. Ichinohe, A. Sekiguchi, Y. Apeloig, *Angew. Chem. Int. Ed.* **2015**, *54*, 12144–12148; *Angew. Chem.* **2015**, *127*, 12312–12316.
[5] O. I. Magidson, *Ber. Dtsch. Chem. Ges.* **1925**, *58*, 433–442.
[6] V. Franzen, H.-I. Joschek, *Justus Liebigs Ann. Chem.* **1961**, *648*, 63–68.
[7] a) A. H. Beck, *Sterisch Gehinderte Doppelbindungssysteme*, Dissertation, Ludwig-Maximilians-Universität München, Germany, **1993**; b) A. H. Beck, R. Gompper, K. Hartmann, K. Yokugawa, *Chimia* **1994**, *48*, 492–493.
[8] J. S. Lee, S. C. Nyburg, *Acta Crystallogr. Sect. C* **1985**, *41*, 560–567.
[9] E. D. Bergmann, E. Fischer, Y. Hirshberg, D. Lavie, Y. Sprinzak, J. Szmuszkovicz, *Bull. Soc. Chim. Fr.* **1953**, 789–809.
[10] P. U. Biedermann, A. Levy, M. R. Suissa, J. J. Stezowski, I. Agranat, *Enantiomer* **1996**, *1*, 75–80.
[11] N. Assadi, S. Pogodin, S. Cohen, I. Agranat, *Struct. Chem.* **2013**, *24*, 1229–1240.
[12] P. U. Biedermann, J. J. Stezowski, I. Agranat, *Eur. J. Org. Chem.* **2001**, 15–34.
[13] A. Cnossen, J. C. M. Kistemacher, T. Kojima, B. L. Feringa, *J. Org. Chem.* **2014**, *79*, 927–935.
[14] W. Zeng, Z. Sun, T. S. Herng, T. P. Gonçalves, T. Y. Gopalakrishna, K.-W. Huang, J. Ding, J. Wu, *Angew. Chem. Int. Ed.* **2016**, *55*, 8615–8619; *Angew. Chem.* **2016**, *128*, 8757–8761.
[15] G. E. Rudebusch, J. L. Zafra, K. Jorner, K. Fukuda, J. L. Marshall, I. Arrechea-Marcos, G. L. Espejo, R. P. Ortiz, C. J. Gómez-García, L. N. Zakharov, M. Nakano, H. Ottosson, J. Casado, M. M. Haley, *Nat. Chem.* **2016**, *8*, 753–759.
[16] L. J. Berliner, J. Reuben, *Biological Magnetic Resonance*, *Vol. 12*, Plenum, New York, **1993**.
[17] The paramagnetic contribution to nuclear relaxivity can be so strong that the NMR resonances become undetectable. However, well-resolved and relatively narrow NMR resonances can be obtained in some systems such as paramagnetic metalloproteins.[18a]
[18] a) A. Bencini, D. Gatteschi, *Electron Paramagnetic Resonance of Exchange Coupled Systems*, Springer, Berlin, **1990**; b) J. E. Wertz, J. R. Bolton, *Electron Spin Resonance*, Chapman and Hall, New York, **1986**.
[19] Y.-C. Hsieh, H.-Y. Fang, Y.-T. Chen, R. Yang, C.-I. Yang, P.-T. Chou, M.-Y. Kuo, Y.-T. Wu, *Angew. Chem. Int. Ed.* **2015**, *54*, 3069–3073; *Angew. Chem.* **2015**, *127*, 3112–3116.
[20] B. C. Streifel, J. L. Zafra, G. L. Espejo, C. J. Gómez-García, J. Casado, J. D. Tovar, *Angew. Chem. Int. Ed.* **2015**, *54*, 5888–5893; *Angew. Chem.* **2015**, *127*, 5986–5991.
[21] For examples of bis- and tris-nitroxides showing only a single signal in the ESR spectrum, see: a) M. Tanaka, K. Matsuda, T. Itoh, H. Iwamura, *J. Am. Chem. Soc.* **1998**, *120*, 7168–7173; b) R. Brière, R.-M. Dupeyre, H. Lemaire, C. Morat, A. Rassat, P. Rey, *Bull. Soc. Chim. Fr.* **1965**, 3290–3297.

[22] "The ORCA program system": F. Neese, *Wiley Interdiscip. Rev. Comput. Mol. Sci.* **2012**, *2*, 73 – 78.
[23] a) A. D. Becke, *Phys. Rev. A* **1988**, *38*, 3098 – 3100; b) A. D. Becke, *J. Chem. Phys.* **1993**, *98*, 5648 – 5652; c) Y. Zhang, W. Yang, *Phys. Rev. Lett.* **1998**, *80*, 890.
[24] A. Schaefer, C. Huber, R. Ahlrichs, *J. Chem. Phys.* **1994**, *100*, 5829 – 5835.
[25] S. Grimme, J. Antony, S. Ehrlich, H. Krieg, *J. Chem. Phys.* **2010**, *132*, 154104.
[26] S. Sinnecker, F. Neese, *J. Phys. Chem. A* **2006**, *110*, 12267 – 12275.
[27] J. Owen, *J. Appl. Phys.* **1961**, *32*, 213S – 217S.
[28] H. Sakurai, H. Tobita, M. Kira, Y. Nakadaira, *Angew. Chem. Int. Ed. Engl.* **1980**, *19*, 620; *Angew. Chem.* **1980**, *92*, 632.
[29] a) J. A. Paulson, D. A. Krost, G. L. McPherson, L. D. Rogers, J. L. Atwood, *Inorg. Chem.* **1980**, *19*, 2519 – 2525; b) D. E. Estes, D. J. Hodgson, *Inorg. Chem.* **1976**, *15*, 348 – 352; c) G. F. Kokoszka, H. C. Allen, Jr., G. Gordon, *J. Phys. Chem.* **1967**, *46*, 3013 – 3019; d) G. F. Kokoszka, H. C. Allen, Jr., G. Gordon, *J. Phys. Chem.* **1967**, *46*, 3020 – 3024.
[30] C. Stroh, P. Turek, R. Ziessel, *Chem. Commun.* **1998**, 2337 – 2338.
[31] R.-M. Dupeyre, A. Rassat, J. Ronzaud, *J. Am. Chem. Soc.* **1974**, *96*, 6559 – 6568.

Received: August 1, 2016
Revised: September 20, 2016
Published online: October 20, 2016

